Biosensors and Bioelectronics 64 (2015) 30–35

Contents lists available at ScienceDirect

Biosensors and Bioelectronics

journal homepage: www.elsevier.com/locate/bios

Label-free and non-contact optical biosensing of glucose with quantum dots

Saara A. Khan [a], Gennifer T. Smith [a], Felix Seo [a,b], Audrey K. Ellerbee [a,*]

[a] E.L. Ginzton Laboratory and Department of Electrical Engineering, Stanford University, Stanford, CA 94305, USA
[b] Advanced Center for Laser Science and Spectroscopy, Department of Physics, Hampton University, Hampton, VA 23668, USA

ARTICLE INFO

Article history:
Received 4 June 2014
Received in revised form
28 July 2014
Accepted 7 August 2014
Available online 22 August 2014

Keywords:
Quantum dot
Biosensor
Glucose
Optical transduction
Hexokinase–glucose 6-phosphate dehydrogenase

ABSTRACT

We present a label-free, optical sensor for biomedical applications based on changes in the visible photoluminescence (PL) of quantum dots in a thin polymer film. Using glucose as the target molecule, the screening of UV excitation due to pre-absorption by the product of an enzymatic assay leads to quenching of the PL of quantum dots (QDs) in a non-contact scheme. The irradiance changes in QD PL indicate quantitatively the level of glucose present. The non-contact nature of the assay prevents surface degradation of the QDs, which yields an efficient, waste-free, cost-effective, portable, and sustainable biosensor with attractive market features. The limit of detection of the demonstrated biosensor is ~3.5 μm, which is competitive with existing contact-based bioassays. In addition, the biosensor operates over the entire clinically relevant range of glucose concentrations of biological fluids including urine and whole blood. The comparable results achieved across a range of cost-affordable detectors, including a spectrophotometer, portable spectrometer, and iPhone camera, suggest that label-free and visible quantification of glucose with QD films can be applied to low-cost, point-of-care biomedical sensing as well as scientific applications in the laboratory for characterizing glucose or other analytes.

1. Introduction

The unique multiplexing and visual readout capabilities of optical detection provide a convenient means to assess a number of important molecules, such as glucose, which is important in public health (Stan et al., 2011), the food industry (Terry et al., 2005), the life sciences (Porterfield, 2007), and other industry sectors. However, many existing techniques for optical detection of glucose suffer from low signal-to-noise (*S*/*N*) or repeatability (e.g., mid-IR transmission spectroscopy and spectrophotometry (Zeller et al., 1989; Bhandare et al., 1993; McNichols and Coté, 2000)), and have low specificity for biological fluids (e.g., polarization-based methods (Malik and Coté, 2009; Solanki et al., 2013)). Raman scattering is a highly specific analysis because it provides a molecule fingerprint; however, it is very hard to measure in biological tissue due to the large background scattering in the visible and near-IR spectral regions and the very weak signal associated with third-order nonlinear optical processes (Shao et al., 2012; Rigo et al., 2011). Surface plasmon resonance (SPR)-based biosensors (Lo et al., 2011) and refractive-index-based detection methods (Wang et al., 2011) have also been demonstrated for quantification of glucose, but SPR-based sensors generally involve irreversible surface activation, and both methods exhibit a decrease in performance in complex media such as urine or blood.

The use of semiconductor quantum dots (QDs) for biomedical sensing is of great interest because QDs with sizes near the bulk Bohr radius exhibit good color purity, high quantum efficiency, and large tunability in the optical spectral region (Rigo et al., 2011; Lo et al., 2011; Wang et al., 2011; Kim et al., 2012). In addition, semiconductor materials can be incorporated into electronic biodevices and can be excited electrically (e.g., QD LED). Nanoscale QDs, moreover, are easily integrated with flexible and portable devices.

Strategies for QD-based sensing of analytes such as glucose can be characterized as either contact or non-contact techniques: we define contact-based strategies (Tan et al., 2013) as those in which the QDs are in direct contact with the analyte-containing solution under test. Unfortunately, contact-based strategies often modify the solubility, aggregation behavior, surface and sensitivity of the QDs in the presence of the analyte. In addition, liquid-phase contact-based QD sensors have limited reusability because QDs having high optical quality cannot be extracted from the mixture solutions. For example, contact-based bioassays using enzymatic reactions have been used to induce fluorescence quenching of QDs via irreversible degradation of the QDs: in these systems the addition of glucose oxidase or horseradish peroxidase leads to

* Corresponding author.

http://dx.doi.org/10.1016/j.bios.2014.08.035
0956-5663/

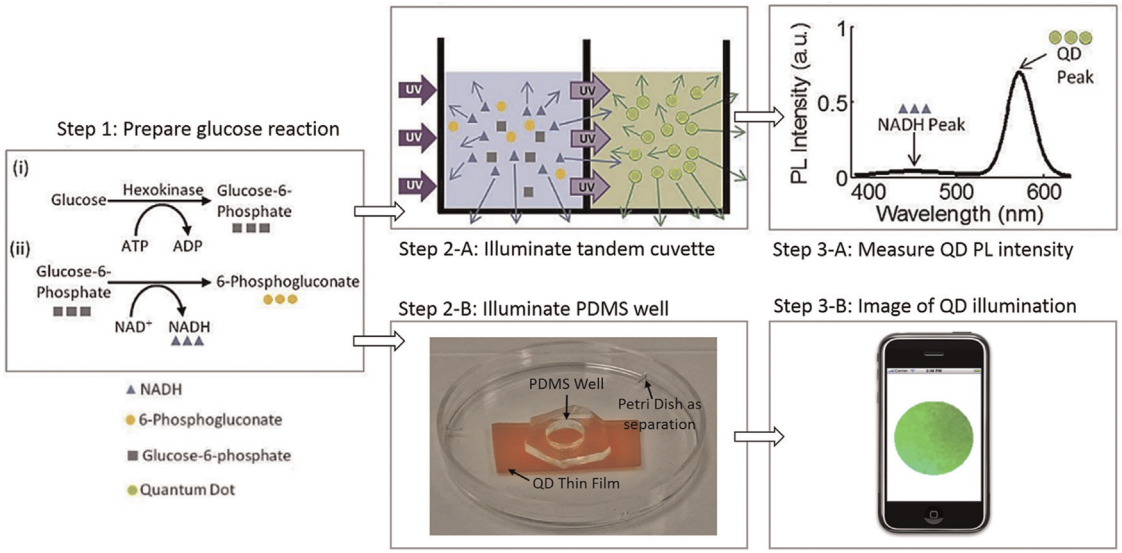

Fig. 1. Illustration of Technique. Schematic illustration of a non-contact optical transduction for the quantitation of glucose with either colloidal quantum dots in a tandem cuvette (route A) or quantum dot thin films (route B). The fluorescent by-product (NADH) of a hexokinase–glucose 6-phosphate dehydrogenase enzymatic glucose assay absorbs UV excitation light, leading to increased NADH fluorescence and reduced QD PL compared to when no glucose is present. The concentration of glucose present is a direct function of the QD PL, which occurs in the visible range. Residual NADH PL does not interfere with the measurement.

production of H_2O_2, and peroxides formed on the QD surfaces degrade its optical properties. Once the assay is completed, the QDs will not have the same quality.

In contrast to the destructive techniques employed by direct contact-based bioassays, several non-contact strategies have been recently demonstrated. These strategies often include film-encapsulated QDs, but also extend to remote optical measurements Ozana et al. (2014). Despite achieving extremely low LOD using expensive, bulky, and heavy optical instrumentation (Kim et al., 2012), these devices have typical detection ranges of 0–4 mM, which is only ~6% of the full clinically relevant range (Wang et al., 2009; Yuan et al., 2012). Therefore, the development of a reusable, cost effective, portable, and user-friendly QD-based biosensor with a large dynamic range of sensitivity represents a formidable challenge.

In this article, we present a novel strategy (Fig. 1) for optical measurement of the concentration of glucose that incorporates the following aspects: (1) An enzymatic assay produces a fluorescent product, NADH, in proportion to the concentration of glucose present. (2) UV light at ~365 nm illuminates the solution under test; NADH absorbs some of this light and the remainder is used to excite CdSe/ZnS core/shell QDs. The photoluminescence (PL) of the QDs is proportional to the transmitted UV light and falls within the linear excitation regime of the enzymes. Therefore, the PL of the QDs indirectly indicates the glucose concentration in the samples. (3) A photodetector (e.g., spectrometer or iPhone 4S cell phone camera) operating in the visible regime quantifies the PL of QDs and reveals the concentration of glucose in biological fluids. Thus, this label-free and biosensor represents a new technique for optical transduction to visible wavelengths that uses the attenuation of UV light through biological samples to excite QD PL in proportion to the amount of glucose present. While this paper specifically demonstrates the technique with glucose, this strategy can be generalized to other biological solutions that absorb in the UV regime as well.

Non-contact optical transduction has several advantages over existing methods: (1) It does not require labels – the QDs intrinsically produce a visible PL upon excitation. (2) It does not require mixing the QDs with the solution under test, which saves on the cost of materials (namely the QDs) and preserves their integrity because the QDs are not degraded by the enzymatic reaction. (3) The fabricated biosensor is reusable and waste-free because the prepared CdSe/ZnS are photostable in polymer films for the given level of excitation illumination, engendering the system with a long performance lifetime. (4) Once the sensors are made, sample preparation is minimal, and the sensor can work with raw biological fluids such as urine and blood without additional processing. (5) The specificity of this method arises from the choice of enzymes, which readily suggests this strategy can be extended to other analytes aside from glucose. (6) The method is general enough to be implemented with any composition or morphology of QDs. (7) The method can be implemented with low-cost detectors such as mobile phone cameras for point-of-care applications.

2. Experimental design

2.1. Chemicals and materials

Hexokinase–glucose 6-phosphate dehydrogenase (HK-G6PDH) enzymes (purchased as “Glucose Assay Reagent”) and glucose were purchased from Sigma Aldrich (St. Louis, MO, USA). Synthetic urine (s-urine) was purchased from Dyna-Tek Industries (Lenexa, KS, USA). Blood samples (Liquichek Diabetes Control – Level 1) were purchased from Bio-Rad (Hercules, CA, USA). Colloidal semiconductor QDs (5.5–6.5 nm) with a carboxyl surface functional group were purchased from Cytodiagnostics (Burlington, Ontario, Canada). The selected QDs were chosen because they display good photostability without photobleaching and minimally aggregate over time, yielding extended shelf-life. Standard-sized polystyrene cuvettes purchased from Fisher Scientific (Waltham, MA, USA) were cut and held together with double-sided tape to create disposable tandem cuvettes (3.67 mm × 7.6 mm).

2.2. Preparation of glucose samples (water, urine, blood)

Various concentrations of glucose from 1 μM to 25 mM in deionized (DI) water or s-urine were prepared as analytes. Whole-blood samples did not contain glucose when purchased. To test the ability of the system to measure glucose concentrations in whole blood, glucose of a specific concentration was first

dispersed in the phosphate buffered saline (PBS) and then mixed with whole blood at a volumetric ratio of 2 μL:198 μL; all blood samples were mixed with the same amount of PBS so that absorption of other components in the blood remained constant across samples. To initiate the glucose–enzyme reaction, 20 μL of the glucose in the base solution (i.e., DI water, blood or s-urine) was mixed with 1 mL of Glucose Assay Reagent (rehydrated with DI water according to manufacturer specifications or with PBS in the case of the blood-base solution). Finally, the samples were reacted for 25 min prior to the measurement.

2.3. Preparation of quantum dot solutions

Solutions of CdSe/ZnS core/shell QDs were prepared by 1:100 dilution (unless otherwise stated) of the stock concentration provided by the manufacturer (5 mg/mL) with DI water. The absorbances of the QDs at various dilutions (1:10, 1:50, 1:100, 1:250, 1:500, 1:1000) are shown in Fig S4 (Supplementary material), which expands on why a 1:100 dilution was found to be optimal for the experiments.

2.4. Preparation of quantum dot thin films

The CdSe/ZnS colloidal nanoparticles were prepared as described in previous work (Seo et al., 2012). The ordinary CdSe QD has a good color purity, wide optical tunability, good photostability, and high quantum yield. However, when placed on a polymer or glass, its optical properties are severely quenched due to surface-trapped state-related energy transfer. The ZnS shell, having a higher optical bandgap than the CdSe core, reduces optical quenching and preserves the material stability of CdSe QDs. To prepare QDs in a polymer film with various thicknesses on the millimeter scale, a stock mixture of PMMA in toluene at ~60 °C was stirred with a magnet for a several hours until the PMMA was completely dissolved in the toluene. PMMA can be easily dissolved in toluene at room temperature, but moderate heating aids in preparation of higher viscosity PMMA in toluene. The stock mixture of PMMA in toluene was cooled to room temperature, mixed in toluene with the QDs, and stirred with a magnet until the QDs were completely mixed in the PMMA. The QD-PMMA mixture in toluene was dried at room temperature for several days in a fume-hood. Finally, high viscosity PMMA in toluene was placed and dried on both sides of the QD-PMMA film to form a protective layer.

2.5. Optical characterization

All absorption spectra were measured using a UV–vis–NIR spectrophotometer (Cary 6000i, Agilent, USA). Absorption spectra were recorded with an integration time of 0.1 s at a scan rate of 600 nm/min. The absorbance offset caused by instrumentation error upon change in the excitation source between the near vis–NIR and near UV spectral regions was corrected by applying a vertical shift. Emission spectra were characterized using a spectrofluorometer (Jobin-Yvon FluorLog-3, Horiba, USA), spectrometer (USB4000-FL, Ocean Optics, USA), or iPhone 4S. For the Jobin-Yvon spectrofluorometer, optical samples were excited at ~365 nm with a slit width of ~1.5 nm. The emission was collected at a scan rate of 2 nm/s and a slit width ~5 nm. For the USB4000 spectrometer, the optical samples were excited by a UV-LED (M365L2-C1, ThorLabs, USA) excitation source at 365 nm and the emission integration time was 300 ms. The same ThorLabs UV-LED was used to excite the samples for the iPhone measurements.

2.6. Measurement of the concentration of glucose

2.6.1. Colloidal quantum dot solutions

To test the performance of the strategy under ideal conditions, samples were examined in a tandem cuvette configuration. One compartment of a custom-fabricated polystyrene tandem cuvette was filled with 800 μL of 50 μg/mL QD solution, which had an emission peak at ~575 nm, while the other compartment contained 800 μL of the analyte solution. The two compartments were physically separated as shown in Step 2-A, Fig. 1. The excitation source illuminated the face of the tandem cuvette containing the glucose–enzyme reaction, while the QD PL was collected using the spectrofluorometer in a right-angle configuration. The emission measurement, therefore, included both the autofluorescence from the NADH produced from the glucose–enzyme reaction and the QD PL. The glucose concentrations were determined by readout from a calibration curve developed from a subset of sample measurements.

2.6.2. Quantum dot films

A non-contact strategy was also applied for testing the glucose samples through optical transduction of UV light into visible wavelengths with QD films. For the assay, a stock solution for each glucose concentration was prepared by mixing a 10-μL sample and 0.5 mL of enzymes. Then, 50-μL of the stock solution was placed on a plastic Petri dish containing a 6-mm-diameter PDMS well with a uniform optical path length across samples. Although the samples could be placed directly on the QD film, we chose to place them in a Petri dish to ensure additional physical separation between the QDs and solution under test and to further emphasize the non-contact nature of the method.

A transillumination scheme was used to deliver UV light to the sample, and the QD emission was collected by A 10x objective lens and measured by the portable spectrometer. for the iPhone measurement, the camera was placed directly beneath the Petri dish, and the High dynamic range option was set to 'off.'

3. Results and discussion

3.1. Optical properties of the glucose–enzyme reaction and QD solution

Ordinary glucose has low absorption in the UV spectral region. As shown in Fig. 2a, the absorbance of glucose in water is almost invariant with concentration (gray lines), and nearly matches the background spectra obtained from a water-filled cuvette (solid black line). In contrast, when enzymes are reacted with the glucose, the absorbance of the glucose–enzyme reaction significantly increases with increasing concentration of glucose as shown in Fig. 2b, which is in agreement with the previous reports (Kiang et al., 1975; Carroll, 1970). The absorbance change with the presence of HK-G6PDH is the key to specificity for the assay. The absorbance is attributed to the presence of NADH, which is a product of the glucose–enzyme reaction. The NADH absorbs photons in UV spectrum, and emits at ~460 nm. The absorbance at ~365 nm has good linearity as a function of the glucose concentration in the clinically relevant regime from 1 to 25 mM. However, the linearity does not hold for concentrations below ~3 μM due to insufficient NADH production at these very low concentrations (no data included).

3.2. Typical measurement results

Fig. 3a shows representative data collected when using the proposed strategy to measure the concentration of glucose in

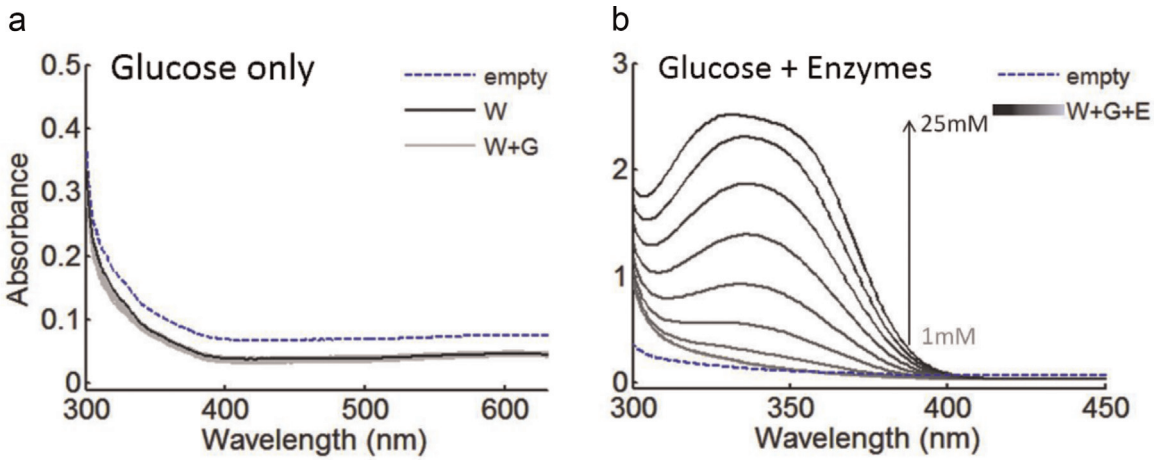

Fig. 2. Absorption spectra (a) Absorption spectrum of an empty cuvette (dashed, blue) and cuvettes with water only (black) or water and glucose (gray) shows that glucose alone does not absorb efficiently in the UV. (b) Absorbance for varying concentrations glucose (1 μM, 2 μM, 2.5 μM, 3 μM, 3.5 μM, 4 μM, 1 mM, 3 mM, 6 mM, 10 mM, 15 mM, 20 mM, 25 mM) increases significantly in the presence of enzymes. W: water; G: glucose; E: enzymes. (For interpretation of the references to color in this figure legend, the reader is referred to the web version of this article.)

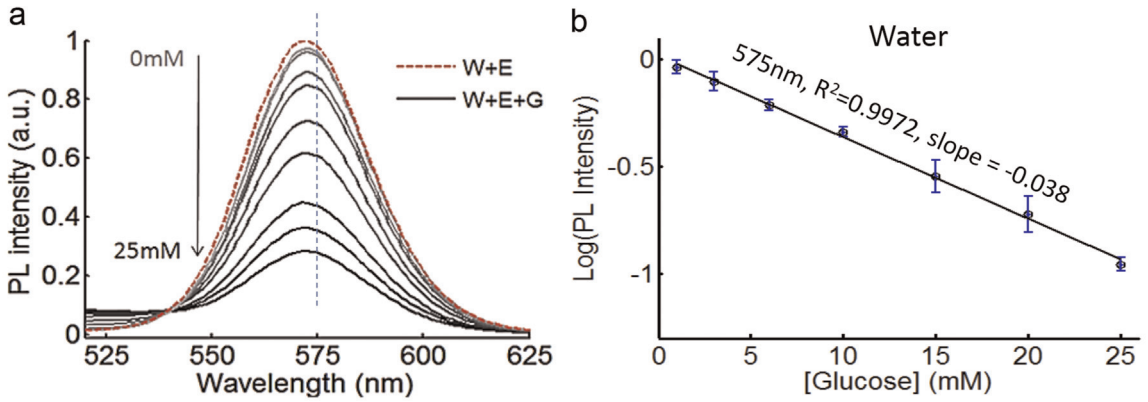

Fig. 3. Typical measurement results. (a) Normalized 575-nm QD PL intensity curves for various concentrations of glucose (3.5 μM, 4 μM, 1 mM, 3 mM, 6 mM, 10 mM, 15 mM, 20 mM, 25 mM). (b) Calibration curves for 575-nm QDs at a 1:100 dilution. Data points correspond to mean ± standard deviation ($n=6$). The curve relates the measured PL intensity to the glucose concentration and is linear when plotted on a log-linear scale. All data are normalized to the PL intensity of a solution containing only water and enzymes (no glucose).

aqueous solution. As expected, the PL intensity of the QDs decreases with increasing concentration of glucose because more NADH is produced from the reaction, leading to higher absorption (i.e., screening) of excitation light and greater reduction (i.e., quenching) of the QD PL emission. As expected for the QDs we chose, the peak wavelength of the PL is ~575 nm.

While the majority of the QD PL we observe is due to excitation with unabsorbed 365-nm source light that reaches the QDs after passing through the sample, it should be noted that a portion of the PL at the peak emission wavelength, when measured in this configuration, is also derived from absorption of the fluorescence emission of the NADH product of the reaction (see Supplementary materials), which is also in range of excitation wavelengths to stimulate QD PL. In brief, QDs are stimulated both from the UV source directly (i.e., unabsorbed excitation light) and the NADH fluorescence. The system is configured such that the UV light source at ~365 nm excites the NADH first (present in the sample) and the QDs next (present in the film or second compartment of the tandem cuvette). Hence, the UV excitation light is initially absorbed by the NADH, which results in some PL; however, the initial absorption by NADH largely results in the screening of the UV excitation illumination to the QDs. Therefore, the degree of quenching of the QD PL depends on the amount of NADH present. The lower limit of detection in aqueous solution was found to be 3.5 μM with an S/N of ~132 where the signal S indicates the PL irradiance of the QD, and the noise N includes the PL irradiance of NADH and background irradiation and illumination; the upper limit of detection exceeds the clinically relevant range (> 22 mM).

Fig. 3b shows a linear curve that relates the glucose concentration to the observed PL at a single wavelength by plotting the PL irradiance at 575 nm on a log-linear scale. The least-squares best fit is R^2~0.9972, as shown in Fig. 3b. A weak red-shift in the PL was observed as the glucose concentration was increased, but this spectral change was ignored for the linearity analysis. Although the NADH fluorescence contributes to the measured PL as described above, it does not affect the results or the linearity of the curve. This was validated through an alternative measurement configuration where the NADH fluorescence was blocked and it was observed that the linearity of the curve persisted.

We compared our typical measurement result to the standard method used for creating calibration curves with UV–vis Absorption Spectroscopy. From Fig. 2b we extracted the data from the absorption spectra at 365-nm and found the calibration curve to have a slope of ~0.0404 with a R^2~0.9994. The sensitivity of the standard method was thus found to be only slightly higher than our method (Fig. 3b, slope ~0.038, R^2~0.9972). While the two methods are similar in terms of sensitivity, the ability to perform biosensing using a visible-wavelength detector can decrease the overall cost and size of the system and may outweigh the benefit of using previous absorption spectroscopy methods.

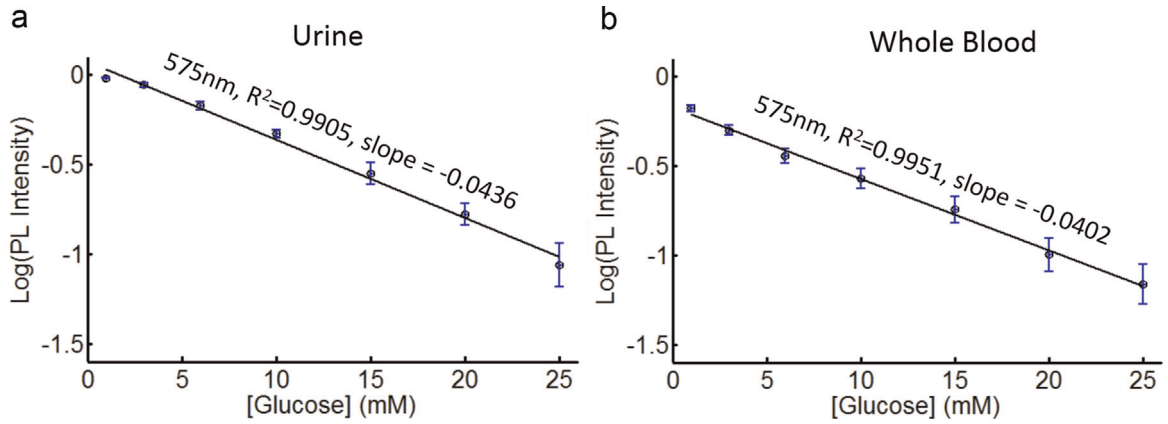

Fig. 4. Calibration curves for biological fluids. Calibration curves for glucose present in (a) urine and (b) whole blood. Data points correspond to mean ± standard deviation ($n=6$).

3.3. Measurement of glucose in biological fluids

The optical transduction scheme was also applied to measure the concentration of glucose in biological fluids by mixing glucose with whole blood or s-urine. In each case, calibration curves with R^2 ~0.9905 and R^2~0.9951 (for urine and blood measurements, respectively) were extracted from data collected from samples with set concentrations of glucose. Then the concentrations of glucose in "test" samples were examined and determined using the calibration curve.

Fig. 4 shows the calibration curves of QD PL irradiance as a function of glucose concentration in urine and blood samples, respectively. For the "test" urine and blood samples, the set-versus-fit lines show the high accuracy obtained based on readout of the calibration curve, as shown in Fig. 5. The slope of the set-fit curve indicates the relationship of the intended versus measured concentrations using the QD sensor. For the urine and blood samples, the set-fit slopes were extracted to be ~0.97 and ~1.016, respectively. The results for the whole blood samples are within the international standards for blood glucose meters (ISO 15197), as shown by the shaded area in Fig. 5b.

3.4. Measurement of glucose with QD thin films

To demonstrate the potential of this strategy to be incorporated into portable diagnostics for point-of-care testing, QD polymer films were utilized to enable facile integration with compact devices such as handheld commercial spectrometers and mobile phone cameras.

3.4.1. Portable spectrometer

Using a handheld spectrometer, the calibration curves for glucose concentrations in water, urine, and blood show strong linearity over the entire medically relevant concentration range from 1 to 25 mM. The results obtained with a portable spectrometer have similar sensitivity (i.e., similar slope) as the results obtained with a research-grade spectrophotometer (Table 1). The transillumination scheme used for this handheld spectrometer (compared to the right-angled collection scheme for the spectrophotometer) offered the additional advantage of no interference from the NADH fluorescence emission, which can otherwise appear as an additional PL peak near 460 nm.

3.4.2. iPhone camera

The compatibility of this strategy with an iPhone camera was also tested by obtaining calibration curves for measuring the concentration of glucose in water, s-urine and whole blood. The iPhone was placed directly beneath the QD film and color images were taken in front-view mode with the camera flash turned off. Raw RGB data from the camera were filtered by color and corrected for ambient light (using the blue color channel) in Matlab. The resulting data consist of the average intensity of light measured by the green imaging channel, in accordance with the green PL peak of the QD-polymer film at ~550 nm. A circular regional selection mask was used to extract only the PL irradiance from the QDs, as shown in Step 3-B, Fig. 1. In general, the slopes of the calibration curve (Table 1) obtained with the iPhone are similar to those with the more expensive instruments (spectrophotometer and handheld spectrometer), but show a slight

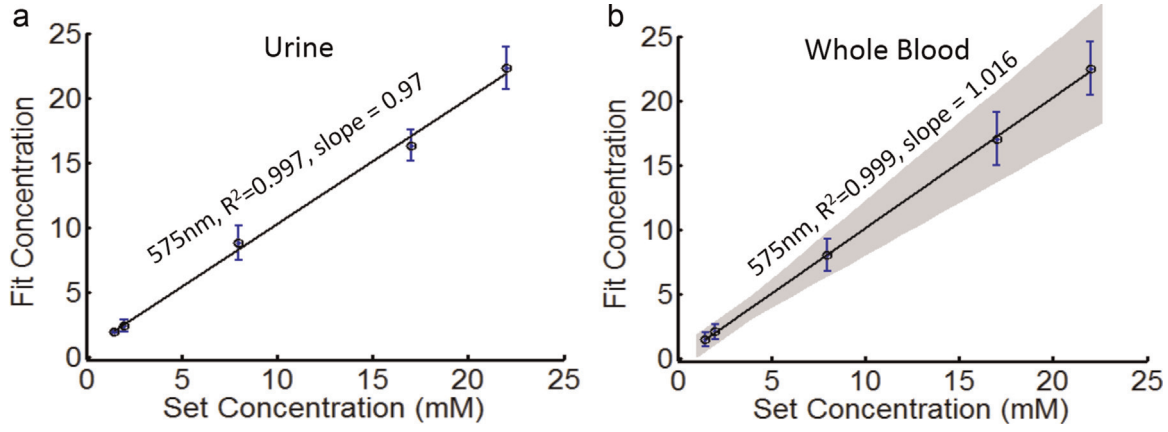

Fig. 5. Sample accuracy for biological fluids. Set versus fit graphs for (a) urine and (b) whole blood. Shaded region in (b) represents the accepted ISO standards for blood glucose meters. Data points correspond to mean ± standard deviation ($n=6$).

Table 1
Results from various measurement devices.

	Spectrofluorometer		Spectrometer		iPhone 4S	
	Slope	R^2	*Slope*	R^2	*Slope*	R^2
Water	−0.048	0.99	−0.026	0.95	−0.024	0.99
Urine	−0.052	0.99	−0.023	0.99	−0.03	0.92
Blood	−0.053	0.99	−0.015	0.96	−0.01	0.94

Results of calibration curves for water, urine, blood among 3 different measurement devices: spectrofluorometer, spectrometer, and iPhone 4S camera. Colloidal QDs at 575 nm were used for Spectrofluorometer and QD films at 550 nm were used for spectrometer and iPhone 4S camera detection.

departure from the values measured with those instruments for the whole blood sample. The discrepancy is due to the fact that the broadband green-pass filter in the iPhone integrates the PL irradiance incident on it for all wavelengths within the pass band. In contrast, the calibration curve extractions using the spectrometers were done at the single wavelength. Nevertheless, the results for all samples with an iPhone cover the entire clinically relevant range with reasonably high value of R^2. This result strongly suggests the viability of label-free, non-contact, and visible quantification of glucose with QD-polymer films via optical transduction for low-cost, user-friendly, and portable optical biosensing.

4. Conclusion

A strategy for characterization of the concentration of glucose via optical transduction of UV excitation light into quenched QD PL at visible wavelengths was demonstrated. The strategy is highly generalizable and can be applied to numerous assays. While absorption-based strategies are not themselves specific, the specificity of such tests can be incorporated through the use of enzymatic assays, as is standard for most electrochemical methods currently used for testing glucose and other analytes (Hilditch and Green, 1991). Previous methods of optical assessment using HK-G6PDH to measure the concentration of glucose based on the absorption of UV light (Kiang et al., 1975; Carroll, 1970; De Courten et al., 2012) are limited by the requirement of having a UV detector. However, the presented work takes advantage of widely available, accessible and portable camera phones with visible-wavelength detectors as a basis for glucose detection, suggesting that a camera phone with an integrated QD film can serve as a next-generation portable, point-of-care public health device. The need for such devices is particularly acute for public health applications in regions in need of low-cost devices. Amid growing interest from other researchers seeking to characterize various samples using mobile phone cameras (Iqbal and Eriksson, 2013), the current work offers a novel concept for non-contact and label-free biosensing, and demonstrated the feasibility of a cost effective, portable, and user-friendly health device using a cell phone camera.

In addition to a proof-of-concept application to measure glucose levels in aqueous solutions, non-contact and label-free biosensing via optical transduction was applied to glucose in more complex biological fluids such as s-urine and blood. Current QD glucose sensors require the user to process blood into serum (Wu et al., 2010; Yuan et al., 2009) or add BSA to whole blood to block non-specific absorption (Hu et al., 2010) before measurements can be taken. The presented strategy does not require processing or dilution of blood or urine samples, is ready to work in clinical settings without additional preparation, and the results were validated to fall within the ranges of accuracy required by the International Organization for Standardization for in vitro blood–glucose monitoring systems (ISO 15197, 2013).

In conclusion, a label-free and non-contact biosensing method based on optical transduction of enzyme-mediated excitation screening and PL quenching of QD films is demonstrated as a viable strategy to measure the concentration of glucose in the visible spectral region with low-cost and point-of-care biomedical sensing as well as scientific applications.

Acknowledgment

This work was supported by Air Force Research Award (FA9550-12-1-0269), Army Research Office (W911NF-11-1-0177), and National Science Foundation (HRD-1137747). The authors' (SAK and GTS) activities were supported by the National Science Foundation Graduate Research Fellowship Program. SAK and GTS thank Jen Dionne and Ashwin Atre for the use of the spectrophotometer, and Kristen Lurie, Tahereh Marvdashti, and Lian Duan for valuable discussions.

Appendix A. Supplementary materials

Supplementary data associated with this article can be found in the online version at http://dx.doi.org/10.1016/j.bios.2014.08.035.

References

Bhandare, P., Mendelson, Y., Peura, R. a., Janatsch, G., Kruse-Jarres, J.D., Marbach, R., Heise, H.M., 1993. Appl. Spectrosc. 47, 1214–1221.
Carroll, J.J., 1970. Biochemical Medicine 180, 171–180.
De Courten, D., Baumann, L., Scherer, L.J., Wolf, M., 2012. Procedia Eng. 47, 1203–1206.
Hilditch, P., Green, M.J., 1991. Analyst 116, 1217–1220.
Hu, M., Tian, J., Lu, H.-T., Weng, L.-X., Wang, L.-H., 2010. Talanta 82, 997–1002.
Iqbal, Z., Eriksson, M., 2013. Sensors and Actuators B: Chemical 185, 354–362.
ISO 15197, 2013.
Kim, S., Seo, J., Ramdon, R., Pyo, H.-B., Song, K., Kang, B., 2012. J. Nanomater., 693575.
Kiang, S.W., Kuan, J.W., Guilbault, G.G., 1975. Clin. Chem. 21, 1799–1801.
Lo, K.-C., Li, C.-T., Yen, T.-J., 2011. 24th Annual Meeting of the IEEE Photonics Society, vol. 5, pp. 931–932.
McNichols, R.J., Coté, G.L., 2000. J. Biomed. Opt. 5, 5–16.
Malik, B.H., Coté, G.L., 2009. SPIE Proc. 7186, 718604–718604–5.
Ozana, N., Arbel, N., Beiderman, Y., Mico, V., Sanz, M., Garcia, J., Anand, A., Javidi, B., Epstein, Y., Zalevsky, Z., 2014. Biomed. Opt. Express 5, 1926–1940.
Porterfield, D.M., 2007. Biosens. Bioelectron. 22, 1186–1196.
Rigo, M., Jaetae, S., Kim, W.-J., Jung, S., 2011. J. Vib. Spectrosc., 57.
Stan, N.G., Con, D., Trial, C., 2011. Diabetes Care 34 (Suppl. 1), S4–S10.
Solanki, J., Choudhary, O.P., Sen, P., Andrews, J.T., 2013. Rev. Sci. Instrum. 84, 073114.
Shao, J., Lin, M., Li, Y., Li, X., Liu, J., Liang, J., Yao, H., 2012. PLoS One 7, e48127.
Seo, J., Fudala, R., Kim, W.-J., Rich, R., Tabibi, B., Cho, H., Cryczynski, Z., Gryczynski, I., 2012. Opt. Mater. Express 2, 1026.
Terry, L. a, White, S.F., Tigwell, L.J., 2005. J. Agric. Food Chem. 53, 1309–1316.
Tan, L., He, X., Chen, D., Wu, X., Li, H., Ren, X., Meng, X., Tang, F., 2013. J. Biomed. Nanotechnol. 9, 53–60.
Wang, J., Banerji, S., Menegazzo, N., Peng, W., Zou, Q., Booksh, K.S., 2011. Talanta 86, 133–141.
Wang, X., Chen, H., Zhou, T., Lin, Z., Zeng, J., Xie, Z., Chen, X., Wong, K., Chen, G., Wang, X., 2009. Biosens. Bioelectron. 24, 3702–3705.
Wu, P., He, Y., Wang, H.-F., Yan, X.-P., 2010. Anal. Chem. 82, 1427–1433.
Yuan, J., Gaponik, N., Eychmüller, A., 2012. Anal. Chem. 84, 5047–5052.
Yuan, J., Guo, W., Yin, J., Wang, E., 2009. Talanta 77, 1858–1863.
Zeller, H., Novak, P., Landgraf, R., 1989. Int. J. Artif. Organs 12, 129–135.